604 *Macromolecules* **2011**, *44*, 604–611
DOI: 10.1021/ma1024544

Macromolecules
ARTICLE

Photoresponse of Complexes between Surfactants and Azobenzene-Modified Polymers Accounting for the Random Distribution of Hydrophobic Side Groups

Juliette Ruchmann,[†] Sarra C. Sebai,*[,‡] and Christophe Tribet[‡]

[†]*UPMC & CNRS UMR 7615, Laboratoire de Physico-chimie des polymères et des milieux dispersés, ESPCI, 10 rue Vauquelin, 75005 Paris, France, and* [‡]*Ecole Normale Supérieure & CNRS UMR 8640, Pôle Chimie Biophysique, 24 rue Lhomond, 75005 Paris, France*

Received October 28, 2010; Revised Manuscript Received December 15, 2010

ABSTRACT: The design of photoresponsive macromolecules has opened the route to many applications, in particular to trigger macroscopic responses induced by light irradiation in complex fluids and polymer−surfactant formulations. In this report, we studied the association of three sets of azobenzene modified polymer (AMPs) derived from poly(acrylic)acid with varying integration levels of azobenzene and various azobenzene hydrophobic moieties, with the neutral surfactant Triton X 100 (TX 100). Binding isotherms in dilute aqueous solutions were determined by spectrophotometry (to measure the fraction of bound azobenzene) and capillary electrophoresis (to measure the amount of bound TX 100). The degree of binding of TX 100 to AMPs increases markedly with increasing azobenzene hydrophobicity and density in AMPs. A noticeable and reversible photoresponse of the associates was observed upon exposure to UV/visible lights, although the magnitude of the UV-triggered photodissociation and blue-triggered association depends on the chemical structure of both the azobenzene and AMPs. We introduce a critical distance l_c that accounts as single parameter for the balance between energy gain of hydrophobic binding and energy loss due to chain conformational constraints. Only segments of chains flanked with two azobenzene groups at their ends and shorter than l_c are assumed to bind tightly. l_c is used to fit both the maximum fraction of azobenzene transferred into TX 100 micelles (with saturation well below 100% despite the presence of excess free TX 100) and the amount of bound TX 100 as a function of the density of azobenzene in the chains. The model includes the effect of random distribution of azobenzene moieties along the chains. From this analysis, we find criterions for optimization of the photoresponse as a function of the azobenzene hydrophobicity and density in the chain, and the chain length.

Introduction

Light-responsive polymers and surfactants are attractive command-molecules for remote control of complex fluids. Such systems have been tailored for many applications, in particular in reversible photoswitching properties including phase transition,[1] gelation[2−4] and controlled release,[5] motion or relief on surfaces,[6] and surface properties including surface tension[7,8] and wettability.[9] The macroscopic responses often rely on phototriggered interactions and assemblies between polymers,[10,11] or polymer and surfactant molecules (either conventional surfactants[12,13] or photoresponsive ones[14−16]). At the molecular scale, the interactions are controlled by photoisomerisation of chromophore groups such as azobenzene. For instance, the trans-azobenzene group (apolar isomer) undergoes a reversible transconvertion into its cis-polar isomer under exposure to UV light. Because of their chemical stability and the versatility of their chemistry, azobenzene derivatives have been tailored for application in all fields cited above, as reviewed in refs 17 and 18.

Here with focus on light-responsiveness of assemblies between azobenzene-modified polymers (AMPs) and surfactants in aqueous solutions. These assemblies transduce the photoresponse achieved at the molecular level and amplify it up to the macroscopic scale. The magnitude of responses shows however a complex relationship between AMPs and surfactants, with composition and structural parameters variation (polymer length and hydrophobicity, density and distribution of side groups, etc.) involved. Because of their large field of applications, polymer/surfactants systems (without sensitivity to light) have been extensively studied (for reviews:[19,20]). The trends and properties achieved upon varying the chemical structures of polymers (e.g., increasing the amount or the length of hydrophobic side groups in chains) are generally well described, though hardly in quantitative terms. Hence, prediction on the magnitude of responses that can be achieved in these systems is difficult. In particular, we wonder whether the photoswitch of azobenzene side groups provides a sufficient drive to trigger macroscopic photoresponses. Therefore, we studied a set of AMPs/surfactant systems as models of choice for a better understanding of the stability of these complexes, and eventually to uncover a matrix of optimized parameters, which are more relevant for the formulation of (highly) light-responsive complex fluids.

We present data on the association between the neutral surfactant Triton X 100 (TX 100) and a homologous set of post-modified poly(acrylic)acid with varying amount of azobenzene side groups, to compare polymers with varying hydrophobicities but with the same parent chain. The hydrophobicity of the azobenzene side groups was also varied by using three different precursor molecules and substituents of various hydrocarbon contents (Scheme 1). In addition, those three groups display various spacer lengths between the azobenzene and the polymer backbone. We accordingly evaluated the effects on binding isotherms and photoresponse of (i) the amount of azobenzene per chain and (ii) the chemical structure of the azobenzene side group.

Binding isotherms of TX 100 on AMPs were characterized by capillary electrophoresis to measure the equilibrium amount of

*Corresponding author.

 Published on Web 01/12/2011

bound surfactants per polymer chain. Binding of azobenzene moieties was studied by spectrophotometry to evaluate the amount of micelle-bound azobenzene, i.e., the intrachain equilibrium between micelle-bound and unbound azobenzene side groups. Data were analyzed with a binding model accounting for the random distribution of azobenzene in the polymer chain and a graphical representation of the model was shown to fit reasonably well to the data.

This binding model is therefore proposed to predict the combined impact of the following experimental parameters: chain length, hydrophobicity of azobenzene side groups, and degree of modification of the chain. Conditions for an optimal response to light are hence discussed on quantitative basis.

Materials and Methods

Materials. Nonionic poly(ethylene glycol) tert-octylphenyl ether surfactant (TX 100) was purchased from Fluka. Except if specified, reagents and solvents for the synthesis of polymers were from Aldrich. Synthesis of amino derivatives of azobenzene, C6azo-NH2[21] and C4azoC4-NH2, is detailed in the Supporting Information. The synthesis and characterization of AMPs (structure shown in Scheme 1) is described in refs 2 and 21. Briefly, random copolymers were obtained by coupling poly(acrylic) acid chains (PAA) with either 4-phenylazoanilin, C6azo-NH2, or C4azoC4-NH2 in *N*-methyl-pyrrolidone in presence of 1.2 equiv of dicyclohexylcarbodiimide. A first PAA (Polysciences, Inc., Warrington) had a number-average molecular weight of 42 000 g/mol and polydispersity index of 2.5. Another parent PAA, with M_n 60 000 g/mol and polydispersity 6, was also used. The integration level of azobenzene (Table 1) was determined by ^{1}H NMR: integration ratios were obtained from peaks at 2.0 ppm (for CH in the main chain), 3 ppm (α-amido CH_2 in the grafted moieties), or 0.5 ppm (end CH_3 in one azobenzene moieties, C4azoC4, cf. Scheme 1), and in the range 7−8 ppm for aromatic protons of the azobenzenes. An additional determination was obtained by UV−visible spectrophotometry. The absorbance of an azobenzene polymer solution can be expressed as a function of its azobenzene integration level, τ, the average molar mass of a monomer, $M = (1-\tau)M_0 + \tau M_{azo}$ (with M_0 the molar mass of sodium acrylate, and M_{azo} the molar mass of the azobenzene-containing monomer), the polymer concentration by weight, c, and the extinction coefficient of the azobenzene moiety ε as

$$A = \frac{\varepsilon l c \tau}{M}$$

where l is the optical path in the cuvette. The extinction coefficient used was 2.32×10^4 L·mol^{-1}·cm^{-1} at 350 nm for the phenylazoanilin and C6azo-NH2 dyes,[21,12] or 2.45×10^4 L·mol^{-1}·cm^{-1} for the C4azoC4 group. Possible residual amount of water (< 10 wt %) in the lyophilized powder of the polymers may introduce a slight bias in the latter estimate, which leads to a possible overestimation of its value in Table 1. AMPs are denoted "*m*_τazo", "*m*_τC6azo" or "*m*_τC4azoC4" depending on the nature of the azobenzene side chain (see Scheme 1), with *m* being the number-average molecular weight of the parent PAA (in kg/mol) and τ the mol % degree of modification. Stock solutions of AMPs and surfactant in NaOH-boric acid buffer (20 mM, pH = 9.1) and 150 mM NaCl were stirred for 24 h in the dark prior to measurements (dark-adapted samples).

Dynamic (DLS) and Static Light Scattering (SLS). Simultaneous dynamic and static laser light scattering were carried out on a Brookhaven system, equipped with goniometer, multiple τ digital correlator, and laser with an output power of 30 mW, at a wavelength of 637 nm. The data were collected at 25 °C and 90° angle. Temperature control within 0.1 °C was achieved using a Julabo F25 refrigerated bath circulator. Sample solutions were prepared by mixing equal volumes of a 2 g/L TX 100 stock solution in buffer, with a 2 g/L polymer stock solution in 20 mM boric acid-NaOH buffer pH 9.2, with 150 mM NaCl, and filtered on 0.2 μm pore size Millex filters (Millipores). Exposure to UV (365 nm) or blue light (470 nm) was performed in situ

Scheme 1. Structures of Amino Derivatives of Azobenzenes "azo", "C6azo", "C4azoC4" (a) and Randomly Modified Polyacrylic acids (AMPs) (b), with y Typically < 6 mol %, x = (100 - y), X = ∅, −$(CH_2)_5$CONH−, or −$(CH_2)_4$−O−[a]

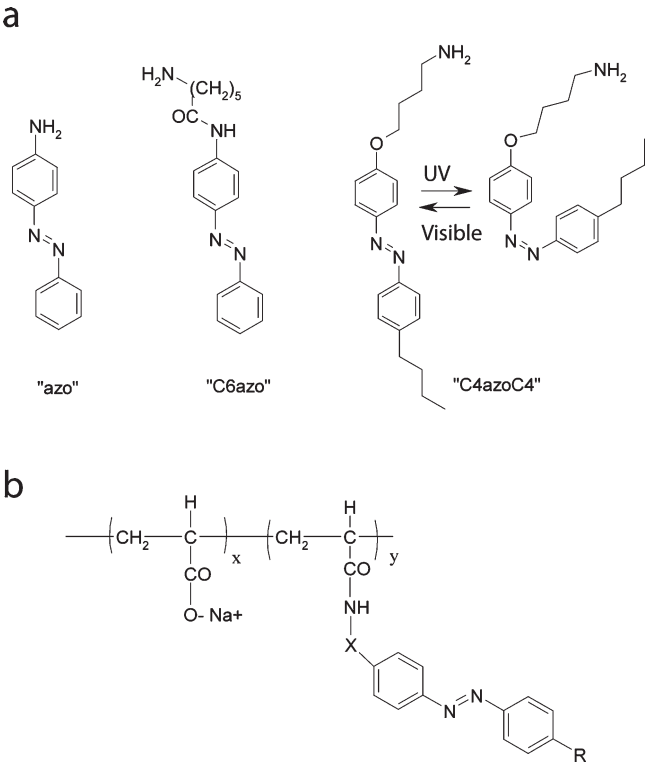

[a] Illustrated with C4azoC4, the apolar isomer (trans) is reversibly converted to the polar cis isomer by exposure to UV light. The photostationary cis/trans ratio depends on the wavelength (~5:1 at 365 nm; ~1:5 at 436 nm).

Table 1. Composition of the Azobenzene-Modified Polyacrylic Acids (AMPs)

		degree of modification (mol %) (τ)		
		from ^{1}H NMR		
	molecular weight (g/mol)[a]	based on protons at 3 ppm	based on aromatic protons	from UV absorbance at 350 nm
42_1C6azo	42 000	1.1 ± 0.1	0.7 ± 0.1	0.9 ± 0.1
60_2.5C6azo	60 000	2.6 ± 0.2	2.1 ± 0.2	2.5 ± 0.2
42_3.5C6azo	42 000	3.4 ± 0.3	3.6 ± 0.3	3.2 ± 0.2
42_5C6azo	42 000	6.1 ± 0.5	4.6 ± 0.4	4.9 ± 0.3
42_1C4azoC4	42 000	0.9 ± 0.1	0.8 ± 0.1	0.7 ± 0.1
42_4.5C4azoC4	42 000	5.0 ± 0.5	3.9 ± 0.2	4.5 ± 0.5
60_1azo	60 000	n.a.	1.4 ± 0.1	0.9 ± 0.1
60_6azo	60 000	n.a.	6.3 ± 0.5	6.1 ± 0.2

[a] Number-average M_n of the parent poly(acrylic acid) under its sodium form.

from a fiber optic placed on the top of the cell (photodiode system CoolLED PE-2, Roper Scientific, France)

Frontal Analysis Continuous Capillary Electrophoresis. Experiments were carried out with a Beckman P/ACE system MDQ instrument equipped with a diode array multiwavelength UV visible detector (Beckman Instruments Fullerton, CA) operating at 25 °C and fitted with bare silica capillaries of 75 μm × 31 cm; effective length: 21 cm (Chromoptic, France). The capillary was flushed daily with 0.1 M NaOH, followed by a water rinse, and finally was allowed to equilibrate with the buffer (20 mM boric acid-NaOH, pH 9.1, 150 mM NaCl). Sample solutions were prepared by mixing aliquots of a 2 g/L TX 100 stock solution in buffer, with 2 g/L polymer stock solution in buffer. The final TX 100 concentration range was 0.05 g/L −1.2 g/L, and the final polymer concentration was 0.2 g/L. Frontal analysis electrophoresis (see ref 21), was carried out using the continuous electrokinetic injection mode against the running buffer, with a positive voltage (3.5 kV) and constant pressure (0.1 psi) applied to the inlet. A first separation was run on the dark-adapted sample, which was thereafter exposed to 365 nm UV light for 20 min (1 mW/cm^2) before being reanalyzed immediately after irradiation. The concentration of free TX 100 was determined from its UV absorbance, using a calibration curve constructed with samples of known concentrations of TX 100 and no polymer.

UV−Visible Spectrophotometry. Absorbance measurements were carried out with a diode array UV−visible spectrophotometer (Evolution Array, Thermo Scientific). A 3 mL sample solution of 0.2 g/L AMPs (in 20 mM boric acid−NaOH buffer, pH 9.1 and 150 mM NaCl) was gradually supplemented by aliquots (typically 15 μL) of the surfactant stock solution at 5 g/L. In order to maintain a stationary fraction of 80% of trans isomer of azobenzene during the experiments, the samples were vertically exposed to visible light (436 ± 10 nm, from a 250 W mercury arc lamp (Oriel) equipped with interference filter). The differential absorption spectra of the samples were obtained by subtracting the spectrum of polymer with no surfactant to the spectrum in the presence of surfactant, after normalization to the dilution factor due to the addition of surfactant. (A UV−vis spectrum is given in the Supporting Information, Figure S1.)

Results and Discussion

Light-Responsive Complexes. Light scattering measurements were carried out to assess the formation of complexes between AMPs and TX 100 (Figure 1). Mixtures of 1 g/L TX 100 and 1 g/L of AMPs (under its dark adapted form) scattered significantly more light than a solution of 1 g/L AMPs and 1 g/L TX 100 separately. In the dilute conditions used here, the scattered intensity was mainly affected by variation of average molar masses of complexes, arising from the binding of TX 100 to the polymer. The association with TX 100 was hence detected by a significant increase in scattering intensities in TX 100/AMPs mixtures (Figure 1), irrespective of side group of the polymers (either azo, C4azoC4, or C6azo). A noticeable feature in Figure 1 is the marked decrease in the scattering intensity after exposure to UV light (365 nm) of the TX 100/AMP mixture, followed by significant recovery of scattering after exposure to blue light (470 nm) in solutions containing azo-modified, C4azoC4-modified, and C6azo-modified chains. These variations illustrate the photodissociation of complexes under UV light and reassociation under blue light. In contrast, the intensity scattered by mixtures of TX 100 and 42_4.5C4azoC4 is less affected by light, suggesting that the nature of the azobenzene chromophore side group plays an important role in the magnitude of the photoresponse. Also light scattering analysis showed that the apparent hydrodynamic radii of the complexes does not change upon exposure to either UV or blue light irradiations and are similar to that of the radius of the polymer with no TX 100

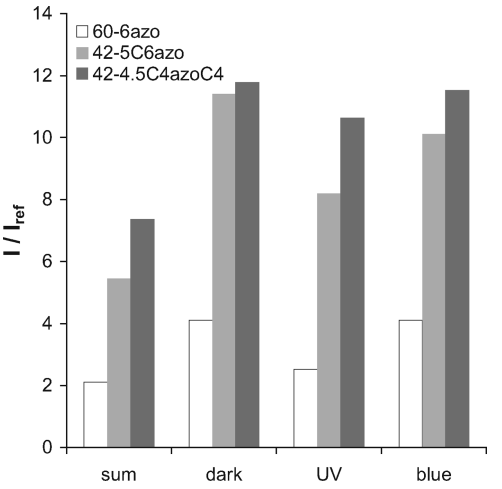

Figure 1. Intensity scattered at 90° angle by solutions of 1 g/L TX 100 and 1 g/L AMPs in 150 mM NaCl, 20 mM boric acid−NaOH buffer pH 9.2, with polymers 60_6azo, 42_5C6azo, and 42_4.5C4azoC4. Key: "sum" represents the sum of intensities scattered by independent solutions of TX 100 and polymer at 1 g/L each; "dark", dark-adapted mixture; "UV", same sample after 2 min exposure under UV light (365 nm); "blue", UV-sample after 2 min exposure to visible light (436 nm). Intensities are normalized by the intensity I_{ref} scattered by toluene.

(ref 22 for examples on C6azo polymers). Here radii in the range 20−30 nm were measured by dynamic light scattering irrespective of the composition of polymer and presence or absence of TX 100 (See Supporting Information, Figure S2). Micelles of TX 100 in absence of polymers have a radius of ca. 4−5 nm, and complexation is accordingly assumed to proceed by "decoration" of long AMPs chains with one or several micelles of TX 100.

Binding of Azobenzene Moiety to Micelles. To evaluate the fraction F_{exp} of bound azobenzene moieties to micelles, we measured by spectrophotometry their spectral shift in solutions of polymers supplemented with TX 100. Results are shown in Figure 2. The transfer of an azobenzene from water to the apolar core of micelles red-shifts its UV−visible absorbance spectrum, resulting in a differential absorbance of the azobenzene in presence and absence of TX 100. The spectral distortion combines the effect of transfer from polar to less polar solvent, which typically induces blue-shifts,[23] and red-shifts due to, e.g., self-assemblies of azobenzenes.[24] In our case, the differential absorbance varies in proportion with the fraction of bound azobenzene chromophore.[12] The differential extinction coefficient of C6azo has been established in[12] and used in eq 1 to estimate F_{exp},. For the sake of simplicity, we used the same equation for C4azoC4 polymers and azo-modified polymers. In practice, UV−vis spectra of C4azoaC4-modified polymers and azo-modifed polymers displayed the same absorption peak in absence of TX 100, although extinction coefficients of the C4azoC4 moieties differ slightly: $\varepsilon_{347\,nm} = 2.32 \times 10^4\ L \cdot mol^{-1} \cdot cm^{-1}$ and $2.45 \times 10^4\ L \cdot mol^{-1} \cdot cm^{-1}$ for C6azo and C4azoC4, respectively.

Therefore, the experimental fraction of bound azobenzene F_{exp} is defined as

$$F_{\exp} = \frac{\mathrm{Abs(TX100)} - \mathrm{Abs(no\ TX100)}}{h\Delta\varepsilon[\mathrm{azobenzene}]} \qquad (1)$$

with $\Delta\varepsilon = 5.1 \times 10^3\ L \cdot mol^{-1} \cdot cm^{-1}$, h the thickness of the cell, [azobenzene] the molar concentrations of azobenzene, Abs() the absorbance at 370 ± 1 nm in presence and absence of TX 100. Figure 2 shows a rapid increase in F_{exp} with increasing concentration of TX 100 occurring above a threshold concentration of TX 100 that is close to its critical

micellar concentration (cmc = 0.1 g/L). At incipient binding, the composition of the surfactant/azobenzene assemblies is however likely to contain a dominant fraction of azobenzene and to vary rapidly with concentrations in samples.[22] The implicit assumption of Beer's law in eq 1 may not be valid if azobenzene moieties form clusters and the value of F_{exp} close to cmc is thus only indicative of the formation of complexes. In contrast, in presence of excess of surfactant (i.e., beyond 0.3 g/L of TX 100 in Figure 2), F_{exp} levels down and slowly reaches a plateau. In this range of composition, the ratio of bound azobenzene per surfactant is low and azobenzene groups are diluted in excess bound TX 100, hence eq 1 should be valid (cf below, the ratio of bound TX 100/polymer reaches up to ~1.6 g/g in presence of excess TX 100, which corresponds to less than two azobenzene groups every 100 molecules of bound TX 100). In order to analyze the binding of AMPs of different compositions, we considered accordingly F_{exp} in the presence of excess TX 100. The parameter quoted F_{max} in Table 2, equals the value of F_{exp} reached at TX 100 of 0.8 g/L, an abscissa somewhat arbitrarily fixed in the plateau region of the data. F_{max} depends markedly on the composition of polymer. The obvious jump of F_{max} upon increasing τ from 1 mol % to 2.5 mol % in C6azo-modified polymers is indicative of a sharp transition between weak binding and tight binding regimes upon increasing the degree of modification of AMPs. The full (100%) binding is however gradually approached with increasing τ. Also in Table 2, comparisons of

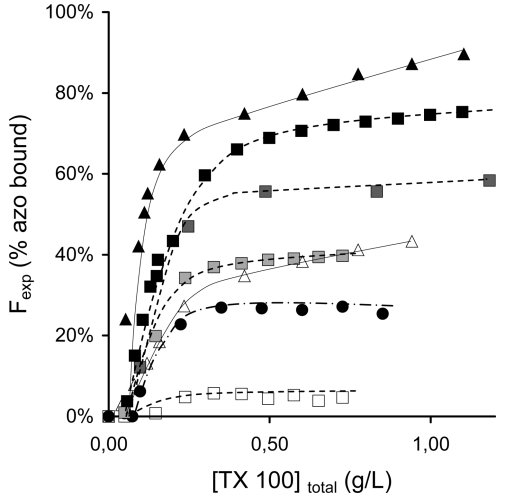

Figure 2. Fraction of micelle-bound azobenzene, F_{exp}, as a function of total TX 100 concentration, as obtained from the variation of absorbance at 370 ± 1 nm and eq 1. Samples were maintained under blue light (436 nm). (●) 60_6azo, (□) 42_1C6azo, (light gray box) 60_2.5C6azo, (dark gray box) 42_3.5C6azo, (■) 42_5C6azo, (△) 42_1C4azoC4, (▲) 42_4.5C4azoC4. All solutions were in 20 mM boric acid-NaOH pH 9.2, 150 mM NaCl. Lines are guide for the eye.

polymers with similar degree of modification show that the degree of association increases with increasing hydrophobicity of the azobenzene in the following order: azo < C6azo < C4azoC4 (N.B. F_{exp} for 60_1azo was too low to be determined). All these features are characteristic properties of hydrophobic associations between surfactants and amphiphilic polymers.

Binding Isotherms of Surfactant into AMPs. Capillary electrophoresis was used to evaluate the binding isotherms, i.e. the amount of polymer-bound TX 100 as a function of concentration of unbound surfactant. Figure 3 shows an abrupt onset of binding at $[TX\ 100]_{free}$ of ca. 0.1 g/L, which is consistent with the above measurements by spectrophotometry. These isotherms also confirm the enhancement of binding upon either increasing the hydrophobicity of the azobenzene side group, or increasing the density of side group of the polymer chains. At concentrations of free TX 100 between 0.1 and 0.2 g/L, we observe on all isotherms a regime of high affinity. In this regime, our measurements show that the amount of bound TX 100 is not markedly dependent on exposure to light. In contrast, in the presence of excess free micelles, which in practice was reached above $[TX\ 100]_{free}$ = 0.2 g/L, the composition of complexes varies markedly less with increasing TX 100 (quasi-saturation) and the association becomes light-responsive. The lack of association below the cmc of the surfactant points out that the binding of AMPs does not markedly perturb micellization of TX 100. Accordingly, in the presence of excess TX 100, the association can be schematically described as a complex of AMP with one or a few micelles of TX 100. The molar mass of TX 100 micelles are of the order of 66 000 g/mol.[25] Association of one micelle on average per chain of AMP thus corresponds to a calculated TX 100/polymer weight ratio of 1 g/g to 1.6 g/g. Table 2 reports the measured amount of bound TX 100 per AMP, in the quasi-saturation conditions, that typically range in the window of 1 g/g to 1.8 g/g in the case of AMPs having the highest hydrophobicities (42_4.5C4azoC4, 42_3.5C6azo, and 42_5C6azo). Some isotherms display a drift in the plateauing regime. The uncertainty of measurement becomes however larger in presence of increasing excess of surfactant, because the amplitude of the signal of bound TX 100 relative to the free ones decreases below 10%. To compare AMPs, irrespective of drifts in the measurements, we determined the binding ratio at the end of the high affinity regime, i.e. at the cross over between the rapid increase in association and the quasi-plateau (cf. lines in Figure 3 A, B).

Model for Critical Segment Hydrophobicity vs Experimental Binding Ratios. The cartoon model conventionally proposed for the binding of surfactant to amphiphilic polymers in dilute solutions is the so-called necklace of micelle-like pearls. Hydrophobic side groups of an isolated macromolecule penetrate the core of surfactant aggregates whose size and properties are similar to those of unbound micelles

Table 2. Characteristic Parameters of Association and Photoresponse

polymer	F_{max} (%)	TX_{bound}:AMP (dark) (g/g)	TX_{bound}:AMP (UV) (g/g)	$l_c\tau$ (spectro)	$\langle L\rangle l_c\tau^2$ (dark)	$\langle L\rangle l_c\tau^2$ (UV)
42_1C6azo	5	0.25	0.08	0.09	0.16	0.03
60_2.5C6azo	38	1.1	0.4	0.28	1.22	0.25
42_3.5C6azo	56	1.3	0.62	0.44	2.25	0.46
42_5C6azo	75	1.4	0.85	0.7	4.87	1.0
42_1C4azoC4	42	0.5	0.2	0.31	0.36	0.12
42_4.5C4azoC4	90	1.8	1.6	15	9.1	3.0
60_1azo	n.d.	0.13	0.08	n.d.	0.06	0.02
60_6azo	27	0.95	0.4	0.16	1.62	0.54

F_{max} is the maximum values of F_{exp} determined from Figure 2, in presence of excess TX 100, as detailed in text ; rows 2 and 3 provide experimental weight ratios of bound TX 100 per (total) AMPs at the cross over regimes shown in Figure 3 ; $l_c\tau$ is determined from Figure 4 and $\langle L\rangle l_c\tau^2$ from Figure 5; n.d., too low to be determined.

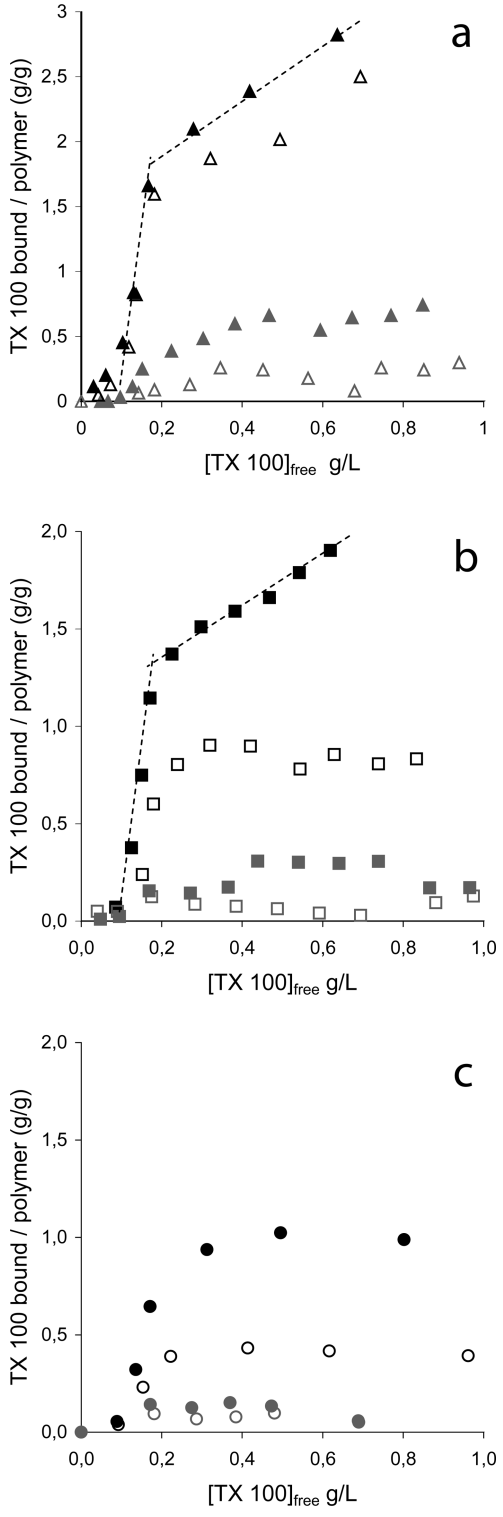

Figure 3. Binding isotherms of TX 100 on AMPs at 0.2 g/L in 20 mM NaOH−boric acid buffer pH 9.2 and 150 mM NaCl. Black and gray symbols are meant for dark-adapted samples, open symbols are for UV-exposed ones: (A) (gray triangle) 42_1C4azoC4, (▲) 42_4.5C4azoC4; (B) (gray square) 42_1C6azo, (■) 42_5C6azo; (C) (gray dot) 60_1azo, (●) 60_6azo.

(Scheme 2). On the basis of this scheme, we propose to identify relevant parameter(s) for optimization of the response to light. In the generally accepted view, association of one (hydrophobic) monomer in a micelle-like cluster competes with steric and entropic loss due to conformational constraints in the backbone. Considering flexible chains and

Scheme 2. Illustration of AMP Multiple Association onto a Hydrophobic Cluster As Controlled by the Balance between the Loop Free Energy and the Free Energy of Transfer of Azobenzene between Water and the Apolar Core upon Light Irradiation

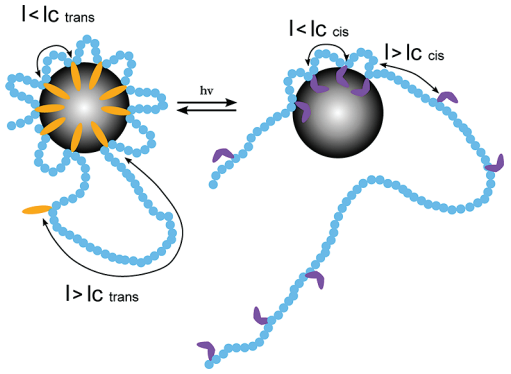

only hydrophobic association (no other significant energy gain due to ionic or hydrogen bond formation) the competition mentioned above comes down to balancing the energy gain from transfer of a hydrophobic monomer from water into the apolar core of a micelle, with the free energy cost of transition from coil to loop conformation of the backbone. Additional loop−loop repulsions may be important in the case of micelles with a dense corona of polymer(s), especially when the polymer hydrophobic grafts dominate the composition of the micelles (e.g., in absence of surfactant or close to critical micellar concentration of the surfactant). The corresponding theory accounting for interloop effect has been developed by Borisov et al.[26,27] Here we will restrain the present purpose to conditions where the energy term arising from interloop interactions can be neglected. In practice, excess micelles and surfactant concentrations well above the critical micellar concentration fulfill these conditions because the number of loops per micelle is low. In this case, Lairez et al.[28] have shown that conformational penalty of a loop is balanced by the energy of transfer (into the micelle core) of the hydrophobes located at both ends of the loop. In the case of flexible neutral chains studied by Lairez, the free energy of loop formation increases monotonously with the length of the loop, which in turn defines a maximal length compatible with the hydrophobes binding. In the same spirit, we define a critical length, l_c, at which the free energy required to fold the loop (i.e., including all the complex coulombic and steric contributions in our case) equals the free energy gain of transfer of the azobenzene end group from water to the micelle-like cluster. Thus, the parameter l_c only depends on the hydrophobicity of an isolated chromophore as measured by its energy of transfer from water to an apolar solvant.

From the remarks above, it is expected that copolymers whose grafting density is over the threshold density of 1 azobenzene every l_c monomers should bind tightly to micelles. The distance between hydrophobic monomers is however polydisperse in synthetic copolymers. We have to account for this practical feature, and include the impact of statistic distributions of hydrophobes on the chains in the model. Random distribution matches with most practical cases of amphiphilic copolymers, in particular with polymers used in the present study.[29] First, we calculate the fraction of azobenzene in an isolated (bound) chain that undergoes association. According to the model above, all segments of the chain shorter than l_c and with azobenzenes at both ends must attach to the micelle and form a loop. Consequently, the fraction F_{azoth} of micelle-bound azobenzene corresponds to the fraction of azobenzene groups that are separated from

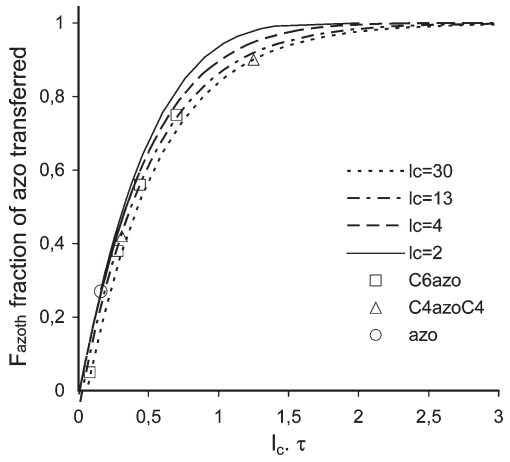

Figure 4. Variation of F_{azoth} with parameters l_c and τ from eq 2 and graphic determination of the product $l_c\tau$ from matching F_{azoth} with F_{max} as given in Table 2. Here $\langle L\rangle = 450$.

another azobenzene by a length smaller than l_c monomers. In a chain of number-average length of $\langle L\rangle$ with an integration level of τ hydrophobes every 100 monomers, F_{azoth} reads as:

$$F_{azoth} = 1 - \frac{\langle L\rangle\tau - 2}{\langle L\rangle\tau}(1-\tau)^{2l_c} - \frac{2}{\langle L\rangle\tau}(1-\tau)^{l_c} \qquad (2)$$

The product $\langle L\rangle\tau$ is the number of hydrophobes (azobenzene) per chain. The first term in eq 2 accounts for the $(\langle L\rangle\tau - 2)$ azobenzene groups located in the middle of the chain and flanked by two azobenzene neighbors distant from each other by a distance bigger than l_c units. Therefore, both segments on their left and right side must display a sequence of l_c successive hydrophilic monomers, which gives the probability of occurrence $(1-\tau)^{2l_c}$. Last term in eq 2 accounts for the two azobenzene groups close to both ends of the chain. They are flanked by one azobenzene group only on one side distant by a segment of minimal length l_c, leaving the other side devoid from hydrophobes (end of the chain). Additional details on eq 2 are provided in the Supporting Information. Finally, F_{azoth} increases rapidly with τ and with l_c, and is weakly sensitive to $\langle L\rangle$ in the window of experimental interest ($\langle L\rangle \sim 450$). Variation of F_{azoth} are plotted in Figure 4 as a function of $l_c\tau$ which enabled us to represent in the same graph the curves representative of experimental range of the parameters l_c, and τ. $\langle L\rangle$ was somewhat arbitrarily fixed to 450 (450 monomers correspond to M_n of 42000 g/mol of the parent poly(acrylic)acid under its sodium form). Except in the window of $l_c\tau$ values between 0.5 and 1.5, differences between the curves in Figure 4 appears of similar magnitude as the uncertainty of measurement of F_{max} obtained from Figure 2. The coordinates ($l_c\tau$, F_{max}), with F_{max} given in Table 2 for each of the various AMPs, were accordingly graphically determined in Figure 4. Self-consistence was achieved by matching the values of τ experimentally determined (as the mean of the values in Table 1) with the position of data points in Figure 4 on the theoretical curve corresponding to the same τ, within uncertainty. Eventually, we evaluated $l_c = 30 \pm 5$ for the C4azoC4 polymers, $l_c = 12 \pm 2$ for the C6azo polymers, and $l_c = 3 \pm 1$ for the azo polymers under their predominantly trans form.

Finally, the gradual increase in association of C6azo polymers with increasing τ is thus fairly compatible with a model assuming 100% binding of the segments of polymer chain whose density is above the critical threshold of two azobenzene every 12 monomers, together with a random distribution of the monomers. The threshold density of binding is found

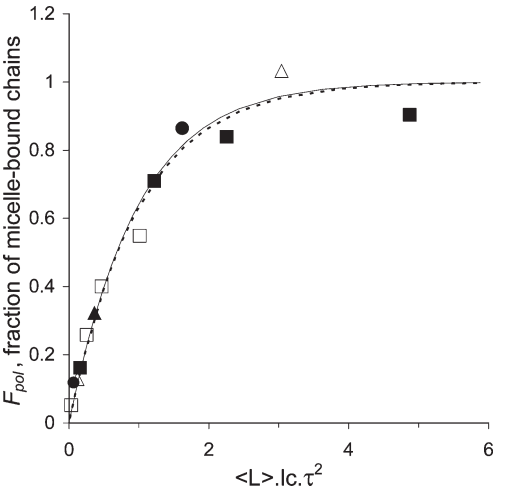

Figure 5. Variation of F_{pol}, the fraction of bound AMP chains in micelles as given by eq 4. Two examples covering the range of experimental parameters are given: dashed line: $\langle L\rangle = 450$, $l_c = 30$; full line $\langle L\rangle = 150$ and $l_c = 2$ and varying τ. Determination of the coordinates of experimental data points obtained from binding isotherms are explained in the text; AMPs modified with (▲, △) C4azoC4, (■, □) C6azo, (●, ○) azo; closed symbols, in the dark; open symbols, exposed to UV.

to decrease with increasing azobenzene side group hydrophobicity.

Variation of l_c upon Trans−Cis Transconversion. Within the same framework, we calculate now the effect of parameters l_c, $\langle L\rangle$, and τ on the amount of bound surfactant in order to evaluate the variation of l_c upon cis−trans isomerization, which may help the optimization of photoresponses. To keep the number of parameters as low as possible, we made several assumptions. First, we restrained the model to conditions of surfactant concentration above cmc and excess micelles equilibrated with bound or free polymer chains. Experimental results shown on Figure 3 showed that the response to light was maximal in this regime, with micelles containing a predominant fraction of TX 100. Then we assumed that when a polymer chain contains at least one segment with a hydrophobicity above the critical threshold value (i.e., a segment shorter than l_c with at least two azobenzene in it), conditions for tight binding are fulfilled with this chain binding to a micelle. The latter assumption simplifies the presumably more gradual transition from weak association to tight association regimes with increasing the number of upper-critical segments in one chain. Finally we did not account here for chain polydispersity in length. Under these assumptions, a chain of total length $\langle L\rangle$ can be decomposed into $\langle L\rangle\tau$ segments of length l_c, each of those beginning with an azobenzene. According to the first hypothesis, a chain composed solely by $\langle L\rangle\tau$ subcritical segments will not bind to a micelle. It is possible to write the probability, P, for a segment of l_c monomers to feature subcritical hydrophobicity as:

$$P = (1-\tau)^{l_c} \qquad (3)$$

Thus, the fraction of micelle-bound chains F_{pol} can be expressed as the complement to 1 of the fraction of chains containing only subcritical segments:

$$F_{pol} = 1 - P^{\langle L\rangle\tau} = 1 - (1-\tau)^{\langle L\rangle l_c\tau} \qquad (4)$$

The influence of parameters l_c and τ on binding is shown in Figure 5. The range of experimentally relevant parameters corresponds to $l_c \sim 1$ to 30, $\tau \sim 1\%$ to 6%, and $L \sim 100-1000$.

The exponent term in eq 4, $\langle L\rangle l_c\tau$, is accordingly well above 1, with τ being significantly smaller than 1. At first approximation, F_{pol} could thus be developed as a polynomial function of $\langle L\rangle l_c\tau^2$. Plotting F_{pol} as a function of the reduced parameter $\langle L\rangle l_c\tau^2$ validates in Figure 5 that a quasi master curve is obtained in the range of experimentally reasonable values of the parameters l_c, τ, and $\langle L\rangle$. This curve enables the comparison between the experimental values of the amount of bound surfactant and calculated ones. Namely, the model assumes the binding of a chain onto an isolated micelle whose properties should be close to micelles of pure TX 100. Hence, the experimental weight ratio, TX $_{\text{bound}}$/polymer, is relied to F_{pol} by:

$$\frac{M_{pol}}{M_{mic}}\frac{\text{TX}_{\text{bound}}}{\text{polymer}} = F_{pol} \qquad (5)$$

with M_{mic} and M_{pol} the molar masses of micelle and AMP of ca. 66 000 and 42 000 g/mol respectively). In the case of dark-adapted samples, experimental ratios were used to place data points in Figure 5 using the values of l_c obtained from spectrophotometry (Table 2, τ given in Table 1, and floating $\langle L\rangle$). Data matched fairly with calculated F_{pol}, irrespective of τ and of the nature of the azobenzene, with a value of $\langle L\rangle$ of 150 $\pm$ 10 (closed symbols in Figure 5, corresponding abscissa in Table 2). We believe that it would be rather delicate to comment on the difference between this value of $\langle L\rangle$ and the number-average $\langle L\rangle$ of ca. 450, especially since the polydispersity of the AMPs is not included in the model. Of more importance to rank the AMPs as a function of binding strength, however, is the amount of bound TX 100 at saturation with various AMPs that matched the theoretical curves in Figure 5 using the parameters τ and l_c measured independently by spectrophotometry.

A value of the reduced parameter $\langle L\rangle l_c\tau^2$ can thus be ascribed to each polymer, either in dark-adapted or UV-exposed conditions. The value of $\langle L\rangle l_c\tau^2$ determined for dark adapted conditions can be divided by $\langle L\rangle l_c\tau^2$ determined in UV conditions to provide the ratio l_c (dark)/l_c (UV) which gives a clear quantification of the photoresponse irrespective of the structural parameters $\langle L\rangle$ and τ. To get an accurate estimation of $\langle L\rangle l_c\tau^2$, for UV-exposed samples, we restricted the analysis to the cases of $F_{pol} < 0.8$ and $\langle L\rangle l_c\tau^2 < 2$, avoiding the plateau region in the theoretical curve. Using $\langle L\rangle = 150$ and the mean values of τ given in Table 1, l_c was floated to fit the data corresponding to UV-adapted sample, and values of the abscissa are reported in Table 2. In the case of C6azo polymers, the same l_c can be used for all the degree of modification (open squares in Figure 5). This analysis finally brings the following ratios of l_c (UV)/l_c (dark): 0.33 for both "azo" and "C4azoC4" AMPs, and 0.21 for C6azo AMPs. These values are of the same order of magnitude. Upon exposure to UV light, the threshold density for binding is typically increased by a factor of 3 to 4, irrespective of the nature of the azobenzene and the degree of modification of AMPs.

Discussion

Altogether, our results bring a consistent picture of conditions of tight hydrophobic association of random amphiphilic copolymers with TX 100 in dilute conditions. Namely, tight surfactant/polymer association is assumed to proceed, without marked change in micellar properties, from the attachment of segments of the chain whose density of azobenzene is above a critical threshold. The assumption of weak or no perturbation of micellar properties is valid in absence of marked stabilization of the micelle upon attachment of the polymer. This may be more frequently occurring with neutral surfactants, in absence of strong interaction between the head groups of the surfactant and the polymer.[30−33] Strong stabilization of surfactant assemblies and comicellization well below the cmc of the surfactant are, for instance, occurring with polymer and surfactant of different charges[34,35] Here, the weak perturbation of surfactant assembling in presence of AMPs is reflected by their lack of effect on the cmc of TX 100. An advantage of our simple binding model is that the composition of complexes can be predicted as a function of molecular and structural parameters such as the polymer length, the average density of modification with hydrophobes, and the threshold density defined by a maximal number of l_c monomers between two hydrophobes undergoing tight associations. Finally, the control of associations between a given pair of AMPs and surfactant partners comes down to the magnitude of variation achieved upon varying l_c.

We now discuss the consequences of the above remarks on the response to stimuli, i.e., on small stimulus-triggered variations of l_c. Stimuli-responsive hydrophobic association is associated here with the effect of light irradiation on azobenzene-modified chains, but it may more generally encompass any variation of the energy of transfer of hydrophobic side groups into micelles under the control of other external conditions that affect l_c (e.g., change in the solvent condition, effect of temperature on water-solubility of polymers, modulation of the ionic charge by pH variation, etc.). In practice, large response to a trans−cis conversion of azobenzene side groups is not easy to achieve and requires tedious synthesis and studies of homologous sets of polymers. The first conclusion drawn from the above analysis is that the polymer architecture is important: sequential distribution of hydrophobes is preferable since a random distribution leads to a broader transition from conditions of no association ($\tau < 1/l_c$) and tight association ($\tau > 1/l_c$). As a second consequence, we note that the amplitude of stimuli-triggered release strongly depends on τ. At high τ a plateau regime is reached (Figures 4 and 5), and no change in the degree of association can be expected upon small stimuli-triggered variation of l_c.

The optimum photoresponse is thus obtained at low τs, when the amount of binding (F_{pol} and F_{azoth}) varies almost linearly with l_c (cf. Figures 4 and 5), which is achieved typically when both $l_c\tau < 1$ and $\langle L\rangle l_c\tau^2 < 2$. In practice, the chemical nature of azobenzene, that affects l_c, is not as easy to modulate as chain length, $\langle L\rangle$, or degree of integration of azobenzene, τ. A procedure for optimizing the photoresponse consists accordingly to screen in a set of AMPs modified with the same azobenzene side group, either decreasing τ, or $\langle L\rangle$, until the above two conditions are reached. The optimal range of τ will depend on the azobenzene side group hydrophobicity, but finally similar degree of sensitivity to the reduced parameters ($l_c\tau$ and $\langle L\rangle l_c\tau^2$) is expected to be reached if τ, or $\langle L\rangle$, is low enough. From this approach, the effect of changing the nature of the azobenzene side group can always be balanced by adjusting the chain length or the density of azobenzene. In addition, we found experimentally that the magnitude of photovariation of l_c does not markedly differ for azobenzene with no spacer ("azo"-modified AMPs), C6azo and C4azoC4 AMPs. This point is reflected by the fact that in each set of AMPs, one example at least showed a photorelease of ca. 50%-60% of bound TX 100 upon exposure to UV (Figure 3A−C). In order to achieve such a high response to UV, one just needs a higher density of azobenzene side groups while decreasing their hydrophobicity; 60−6azo, 42−2.5 C6azo, and 42−1C4azoC4 display accordingly similar magnitude of response. Increasing chain length is expected to produce similar effect as increasing l_c (this is translated in the abscissa of Figures 4 and 5 by the product $\langle L\rangle l_c$), but this point is not validated yet and deserves future investigations. Making longer chains is however likely to favor associations, since the probability to have at least one segment of high local density of azobenzene increases with the chain length in random copolymers.

It may be desirable to lower the degree of modification of the chains and to use low concentrations of azobenzene. For instance, the absorbance of samples must be low enough to permit penetration of light deep into the materials. For millimeter-thick systems, a concentration of azobenzene below one millimolar should hence be preferred (accounting for extinction coefficient of azobenzene of the order of 10^4 $L \cdot mol^{-1} \cdot cm^{-1}$). Conventional application of surfactant/polymer mixtures as emulsifiers, or in gelation and viscosity control, typically requires a few weight percent polymers in solutions, and the upper limit of millimolar concentration of azobenzene are thus corresponded to degree of modification typically lower than 1 mol %. In this case, our analysis pleads in favor of azobenzenes imparted with high hydrophobicity (e.g., by alkyl substituents like in C4azoC4) grafted on long chains at low density of modification.

Conclusion

We have studied the association of three sets of azobenzene-modified copolymers (AMP), bearing photochromes with different hydrophobicities, with TX 100. Our results show that the degrees of binding of both TX 100 (amount of bound surfactant per AMP) and azobenzenes (maximal fraction of bound azobenzene) increase with increasing hydrophobicity and density of azobenzene in AMPs. A marked and reversible response to trans−cis isomerization can be achieved under exposure to UV/visible lights, with up to 50−60% of the dark-bound TX 100 being released under UV light. However the magnitude of photoresponse of AMP:TX 100 complexes and the composition of complexes markedly depends on the chemical structure of both the azobenzene and AMPs. A simple model of binding that takes into account the varying hydrophobicity of the diverse azobenzene and their random distributions in AMPs is proposed. On the basis of the assumption that tight association takes place on polymer segments whose density of azobenzene is above a threshold value, the degrees of (tight) binding are written as a function of three molecular and structural parameters: the average polymer length $\langle L \rangle$, the average density of modification of AMP, τ, and the threshold density as defined by l_c, the maximal number of monomers between two hydrophobes undergoing tight association. Experimental results on the fraction of bound azobenzene and the amount of bound TX 100 are fitting with this model. On this basis, it is shown that isomerization under UV exposure to the cis azobenzene increases the threshold density (decrease in l_c). Optimization of the amount of association/release and of the photoresponse can accordingly be predicted from our model. Interestingly, the magnitude of decrease in l_c that was experimentally achieved points out that photovariation of l_c does not differ significantly among the azobenzene bearing different substituents (i.e., having different hydrophobicities). We conclude that τ can always be adjusted depending on l_c (i.e., here on the hydrohobicity of the azobenzene derivative) in order to get similar responses to light irrespective of the chemical nature of the azobenzene. A more hydrophobic azobenzene requires lower τ, which has the important consequence to lower the concentration of azobenzene used in practice and therefore help the design of photoactive material imparted with low absorbance.

Acknowledgment. This work was supported by the Agence National de la Recherche France for the award of Grant No ANR BLAN 0278-01 and the European Network of Excellence (FP6 NOE "SoftComp" Soft Matter Composite) for financial support. The authors would like to thank I. Iliopoulos and L. Leibler for helpful suggestions.

Supporting Information Available: UV−visible absorption spectra, distribution of AMPs hydrodynamic radii, synthesis and characterization of amino derivatives of azobenzenes, ^{1}H NMR spectra, and calculation of the fraction of tightly bound hydrophobes. This material is available free of charge via the Internet at http://pubs.acs.org.

References and Notes

(1) Irie, M. *Adv. Polym. Sci.* **1993**, *110*, 49–65.
(2) Pouliquen, G.; Tribet, C. *Macromolecules* **2006**, *39*, 373–383.
(3) Tomatsu, I.; Hashidzume, A.; Harada, A. *Macromolecules* **2005**, *38*, 5223–5227.
(4) Sugiura, S.; Szilagyi, A.; Sumaru, K.; Hattori, K.; Takagi, T.; Filipcsei, G.; Zrinyi, M.; Kanamori, T. *Lab Chip* **2009**, *9*, 196–198.
(5) Alvarez-Lorenzo, C.; Bromberg, L.; Concheiro, A. *Photochem. Photobiol.* **2009**, *85*, 848–860.
(6) Katsonis, N.; Lubomska, M.; Pollard, M. M.; Feringa, B. L.; Rudolf, P. *Prog. Surf. Sci.* **2007**, *82*, 407–434.
(7) Eastoe, J.; Dominguez, M. S.; Wyatt, P.; Beeby, A.; Heenan, R. K. *Langmuir* **2002**, *18*, 7837–7844.
(8) Shang, T. G.; Smith, K. A.; Hatton, T. A. *Langmuir* **2003**, *19*, 10764–10773.
(9) Lim, H. S.; Han, J. T.; Kwak, D.; Jin, M.; Cho, K. *J. Am. Chem. Soc.* **2006**, *128*, 14458–14459.
(10) Jochum, F. D.; Theato, P. *Chem. Commun.* **2010**, *46*, 6717–6719.
(11) Tong, X.; Wang, G.; Soldera, A.; Zhao, Y. *J. Phys. Chem. B* **2005**, *109*, 20281–20287.
(12) Khoukh, S.; Oda, R.; Labrot, T.; Perrin, P.; Tribet, C. *Langmuir* **2007**, *23*, 94–104.
(13) Howley, C.; Marangoni, D. G.; Kwak, J. C. T. *Colloid Polym. Sci.* **1997**, *275*, 760–768.
(14) Lee, C. T.; Smith, K. A.; Hatton, T. A. *Macromolecules* **2004**, *37*, 5397–5405.
(15) Ma, N.; Wang, Y. P.; Wang, B. Y.; Wang, Z. Q.; Zhang, X.; Wang, G.; Zhao, Y. *Langmuir* **2007**, *23*, 2874–2878.
(16) Bradley, M.; Vincent, B.; Warren, N.; Eastoe, J.; Vesperinas, A. *Langmuir* **2006**, *22*, 101–105.
(17) Ercole, F.; Davis, T. P.; Evans, R. A. *Polym. Chem.* **2010**, *1*, 37–54.
(18) Zhao, Y.; Ikeda, T. *Smart Light-Responsive Materials: Azobenzene-Containing Polymers and Liquid Crystals*; Wiley: New York, 2009.
(19) Goddard, E. D. In *Principles of Polymer Science and Technology in Cosmetics and Personal Care*; Goddard, E. D., Gruber, J. W., Eds.; Marcel Dekker: New York, 1999; pp 113−180.
(20) La Mesa, C. *J. Colloid Interface Sci.* **2005**, *286*, 148–157.
(21) Pouliquen, G.; Amiel, C.; Tribet, C. *J. Phys. Chem. B* **2007**, *111*, 5587–5595.
(22) Ruchmann, J.; Fouilloux, S.; Tribet, C. *Soft Matter* **2008**, *4*, 2098–2108.
(23) Hutchings, M. G.; Gregory, P.; Campbell, J. S.; Strong, A.; Zamy, J. P.; Lepre, A.; Mills, A. *Chem.—Eur. J.* **1997**, *3*, 1719–1727.
(24) Labarthet, F. L.; Freiberg, S.; Pellerin, C.; Pezolet, M.; Natansohn, A.; Rochon, P. *Macromolecules* **2000**, *33*, 6815–6823.
(25) Molina-Bolivar, J. A.; Aguiar, J.; Ruiz, C. C. *J. Phys. Chem. B* **2002**, *106*, 870–877.
(26) Borisov, O. V.; Halperin, A. *Curr. Opin. Colloid Interface Sci.* **1998**, *3*, 415–421.
(27) Borisov, O. V.; Zhulina, E. B. *Macromolecules* **2005**, *38*, 2506–2514.
(28) Lairez, D.; Adam, M.; Carton, J. P.; Raspaud, E. *Macromolecules* **1997**, *30*, 6798–6809.
(29) Magny, B.; Lafuma, F.; Iliopoulos, I. *Polymer* **1992**, *33*, 3151–3154.
(30) Diab, C.; Winnik, F. M.; Tribet, C. *Langmuir* **2007**, *23*, 3025–2035.
(31) Miyazawa, K.; Winnik, F. M. *J. Phys. Chem. B* **2003**, *107*, 10677–10682.
(32) Johnson, K. M.; Fevola, M. J.; Lochhead, R. Y.; McCormick, C. L. *J. Appl. Polym. Sci.* **2004**, *92*, 658–671.
(33) Sarrazincartalas, A.; Iliopoulos, I.; Audebert, R.; Olsson, U. *Langmuir* **1994**, *10*, 1421–1426.
(34) Magny, B.; Iliopoulos, I.; Zana, R.; Audebert, R. *Langmuir* **1994**, *10*, 3180–3187.
(35) Piculell, L.; Guillemet, F.; Thuresson, K.; Shubin, V.; Ericsson, O. *Adv. Colloid Interface Sci.* **1996**, *63*, 1–21.